Observational Basis for Standard Big Bang Nucleosynthesis and Modeling in PRIMAT

Catherine Slaughter

1. INTRODUCTION

Big Bang Nucleosynthesis (BBN) is the process by which the primordial abundances of light elements in the Universe came to be immediately following the Big Bang. The study of BBN is a multi-subfield endeavor. BBN serves as one of the observational "pillars" of Big Bang Cosmology, is modeled based on an understanding of nuclear and particle physics, and is confirmed through astronomical observation. Many subfields such as stellar astrophysics, galactic archaeology, etc. utilize the findings of BBN research when studying the abundances and metallicities of different celestial bodies and structures. Because of its wide applicability, it is crucial that BBN models and related observationally obtained values are within good agreement. There are four primary products of BBN that are crucial to any BBN model (see sec.3,4,5,6). Their observational and modeled values are in good agreement for three of the four. A Schramm plot (fig. 1), is a useful way of showing modeled BBN abundances compared to their observational values, over a range of the present-day baryon-to-photon fraction ("baryon abundance"), η.

Fig.1 is an output from one of the leading BBN modeling programs, PRImordial MATter (PRIMAT). PRIMAT is a Mathematica notebook developed to model BBN. At the time of writing this paper, it has been cited in over 130 astronomical and cosmological papers, according to ADS. A more extensive overview and example for use of PRIMAT can be found in sec.7.

2. STANDARD BIG BANG NUCLEOSYNTHESIS

Standard Big Bang Nucleosynthesis (SBBN) assumes space is governed by ΛCDM cosmology, based on the Friedmann-Lemaî tre-Robertson-Walker (FLRW) metric. It assumes Einstein gravity, and the Standard Models of particle and nuclear physics. These assumptions–along with high-precision values obtained for the baryon abundance, η (Planck Collaboration et al. 2020)–yield a theory for BBN that

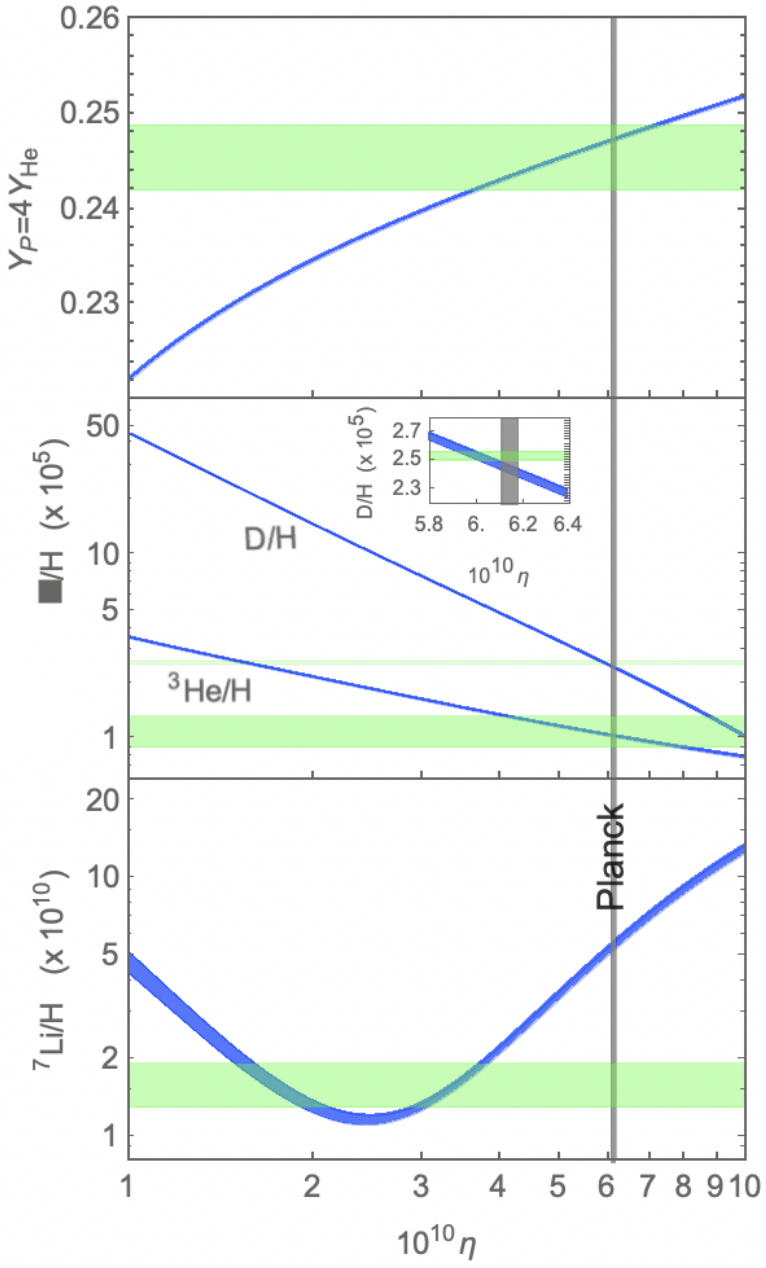

Figure 1. A Schramm plot showing the modeled (blue) and observed (green) values of the four significant nuclei over a range of η. The helium-4 abundance is on top, the deuterium and helium-3 abundances in the middle, and the lithium-7 abundance is on the bottom. Note the different scales on the y-axes. The vertical gray line represents the observed value for η obtained by Planck Collaboration et al. (2020).

contains basically no free parameters. Another example being the number of presumed light neutrino flavors, which is set by the Standard Model at $N_\nu = 3$ (Cyburt et al. 2016).

SBBN starts with protons and neutrons, the constituent particles that make up atomic nuclei. According to the cosmological theories utilized by SBBN, it is safe to assume that, at the time of nucleosynthesis, the Universe was overwhelmingly radiation-dominated. Around this time, the Universe was relatively very hot ($T > 1MeV$). The high temperature meant that the weak (β) interactions that convert protons to neutrons and vice versa where in equilibrium (Cyburt et al. 2016).

$$n \leftrightarrow p + e^{-} + \bar{\nu}$$

$$\nu + n \leftrightarrow p + e^{-}$$

$$e^{+} + n \leftrightarrow p + \bar{\nu}$$

At these temperatures, the dominant (radiation) component of the energy density of the Universe is

$$\rho = \frac{\pi^2}{30}(2 + \frac{7}{2} + \frac{7}{4}N_\nu)T^4,$$

which takes into account the contributions of photons, electrons (and positrons), and neutrinos (where N_ν is the number of neutrino flavors). Soon after, as the Universe expanded and cooled, it reached a point of freeze-out. Physically, freeze-out has two equivalent meanings. Freeze-out occurs when the average time for a weak interaction to occur becomes greater than the age of the Universe or, equivalently, when the interaction rate becomes less than the expansion rate ($\Gamma_{wk} < H$). The temperature at which freeze-out occurs (T_f), also known as the "freeze-out condition" can be found with

$$G_F^2 T^5 \approx \Gamma_{wk}(T_f) = H(T_f) \approx G_N^{1/2} T^2,$$

where G_F is the Fermi constant and G_N is the Newton constant (Cyburt et al. 2016). Solving for T shows that the freeze-out of relative neutron and proton abundances occurs at $T_f \approx 0.8MeV$. From here the neutron to proton ratio can be calculated by the Boltzmann factor

$$(n/p)(T_f) \approx e^{-(m_n - m_p)/T_f} \approx 1/5. \quad (1)$$

This value decreases to about 1/7 due to β-decay between the time of freeze-out and the beginning of nucleosynthesis (Cyburt et al. 2016). From here, these constituent nucleons can begin to form larger ions.

3. DEUTERIUM CREATION AND ABUNDANCE

3.1. *Mechanisms*

Once the Universe reached a point of freeze-out, the first phase of nucleosynthesis was the creation of deuterium nuclei (also known as ${}^2H$ or Hydrogen-2). It should be noted that singular protons are also hydrogen nuclei, and some literature will refer to them as such. The primary nuclear reaction to create deuterium involves the collision of a proton and a neutron (Davids 2020).

$$p + n \rightarrow \gamma + {}^2H$$

It is important to note that for some time after freeze-out, there were a significant number of photons in the Universe with an energy greater than the binding energy of deuterium. From $T \approx 0.8MeV$ to $T \approx 0.1MeV$, much of the deuterium produced was quickly split again. This is referred to as the "deuterium bottleneck." The bottleneck means that nucleosynthesis was limited to the creation of deuterium until the Universe cooled to $T \approx 0.1MeV$, at which point the deuterium lasted long enough to form larger nuclei (Cyburt et al. 2016).

3.2. *Observational Values*

One way to try to observe the primordial deuterium abundance is using extremely low metallicity absorption regions. These are far-away areas of gas and dust with particularly high column densities that are backlit by some very bright, near-blackbody light source (usually, a quasar). By measuring and analyzing the absorption spectrum, the metallicity of the region can be determined (where, in this context, "metal" refers to the astronomical definition, aka anything heavier than helium). The metallicity is crucial in determining whether the region being studied has been injected with metals via stellar nucleosynthesis. If this is the case, the observed deuterium abundance in the region may be tainted. If the metallicity is reasonably low, however, it can be assumed that stellar nucleosynthesis

has not greatly impacted the elemental abundances in the region, and an observational estimate for the primordial deuterium abundance can be made. This is especially true, as deuterium is not formed in stellar nucleosynthesis. This estimate is calculated by looking for variation in the Lymann-α forest of the absorption spectrum that is created when the hydrogen-1 column density of the region is sufficiently high.

Such an estimation was made in Cooke et al. (2018). Using the HIRES echelle spectrograph with upgraded, ultraviolet-sensitive detector, they observed an absorption system in the direction of quasar Q1243+307. The system in question sits at redshift $z_{abs} = 2.52564$, and is measured to have a relative oxygen abundance of $[O/H] = -2.769 \pm 0.028$.[1] The ^1H column density of the region is on the order of 10^{19}, damping the Lyα emission enough to model and calculate an abundance. They find that the region in question as a deuterium abundance of $log_{10}(D/H) = -4.622 \pm 0.015$. This is the seventh in a series of similarly high-quality measurements made by the group. Combining all seven measurements gives a final estimated primordial deuterium abundance of $log_{10}(D/H)_P = -4.5974 \pm 0.0052$ or, on a linear scale[2], $10^5(D/H)_P = 2.527 \pm 0.030$. In doing so, they also find no correlation between the seven D/H values and [O/H], further indicating that their estimate corresponds with the primordial abundance. This is confirmed with modeling in PRIMAT. Looking at the middle frame in fig.1 (and, in particular, the zoomed-in section), it is clear that the observed D/H matches the modeled value with great precision at the assumed η as found in Planck Collaboration et al. (2020).

4. HELIUM-3 CREATION AND ABUNDANCE

4.1. *Mechanisms*

Once deuterium is created and the temperature bottleneck passed, heavier-than-hydrogen nuclei start to form. There is some formation of tritium (^3H) as well. However, this isotope of hydrogen is radioactive, with a half life of ≈ 12.3 years (Lucas et al. 2000). Its short half-life makes it impossible

[1] This is calculated as $[O/H] = log_{10}(\frac{(N_o/N_H)_{star}}{(N_o/N_H)_\odot})$, so the region has an oxygen abundance $\approx 1/600$ that of the Sun.
[2] This is the D/H value used by PRIMAT for comparison purposes.

to estimate a primordial tritium abundance with astronomical observation, so it is not useful in checking BBN models.

There are two primary possible nuclear reactions that would have lead to the creation of ^3He at the time of BBN, both of which require deuterium. The first involves the collision of a deuterium nucleus and a proton, the second is the collision of two deuterium nuclei (Davids 2020).

$$d + p \rightarrow {}^3He + \gamma$$

$$d + d \rightarrow {}^3He + n$$

4.2. *Observational Values*

It is considerably more difficult to obtain an observed primordial abundance for ^3He compared to the three other significant isotopes for BBN modeling. Typically, ^3He general abundances are found by observing the 8.665 GHz spin-flip transition line from HII regions and nebulae. Rood et al. (1998) finds that the measured ^3He abundances appear the same when observing several relatively diffuse HII regions in the galaxy, even if their metallicities otherwise differ. This lack of correlation between ^3He and [O/H] is called the "^3He plateau." Additionally, when observing planetary nebulae, they are able to determine that stellar fusion processes do not lessen the amount of ^3He present in the ISM. In fact, by comparing the abundances of ^3He in the HII regions and planetary nebulae, they conclude that stellar nucleosynthesis increases the abundance of ^3He by a very slight, but nonzero, amount. The ^3He plateau observation, combined with the only slight increase in abundance due to stellar nucleosynthesis, indicate that a hard upper limit on the primordial abundance can be set at the plateau value.

A more recent paper, Bania et al. (2002), finds the value of the plateau with higher precision. Using both the NRAO 140ft telescope and the Max-Planck-Institut fuér Radioastronomie (MPIfR) 100m telescope, they observed 21 "simple" (having simple density and ionization structures) HII regions. They find a hard upper limit (plateau value) of $10^5(^3He/H)_P < 1.9 \pm 0.6$. A softer[3] upper limit is proposed based on the observation of HII region S209, a simple region with large radius from the

[3] "Softer" because the value is obtained by observing only one HII region.

galactic center (and therefore lower metallicity). Their observations totaled 133 hours over 15 years, and found an upper limit[4] of $10^5(^3He/H)_P < 1.1 \pm 0.2$.

5. HELIUM-4 CREATION AND ABUNDANCE

5.1. *Mechanisms*

The primordial ^4He abundance (Y_p) is one of the more useful measures of a BBN model's validity. This is because, to first order, when the deuterium bottleneck breaks up, basically all the existing neutrons get put into ^4He nuclei. From here, it is relatively simple to predict the expected primordial ^4He abundance (Cyburt et al. 2016)

$$Y_p = \frac{2(n/p)}{1 + (n/p)} \approx 0.25,$$

Where $(n/p) \approx 1/7$ (See eq.1 and subsequent paragraph). The ease of this prediction, combined with the fact that the expected primordial ^4He abundance is several orders of magnitude greater than any of the other BBN products, makes Y_p especially useful in testing models.

There are a few ways in which ^4He (sometimes denoted as α) is formed in BBN. The first, and more significant, method involves the collision of a ^3He and a deuterium nucleus. The second involves the collision of a deuterium and a ^7Be (sec.6.1) nucleus.

$$^3He + d \rightarrow {}^4He + p$$

$$d + {}^7Be \rightarrow 2^4He + p$$

It should be noted that the creation of ^7Be requires one ^4He α-particle (sec.6.1). However, the reaction above creates two ^4He nuclei for every ^7Be nucleus, so it remains a valid formation path for ^4He.

5.2. *Observational Values*

While ^4He is incredibly important for testing BBN models, gaining precise observational values of its primordial abundance has historically been difficult. Generally, ^4He abundances are obtained

[4] This is the ^3He/H value used by PRIMAT for comparison purposes.

using observations of relatively metal-poor extragalactic HII regions. By measuring a number of hydrogen and helium emission lines, models of the emission from these regions are generated via Markov Chain Monte Carlo analysis, and individual ^4He abundance estimates are obtained. From here, the ^4He abundances can be modeled as a function of HII region metallicity ([O/H]), and the model equation is extrapolated back to very low metallicity to determine a primordial abundance estimate. Traditionally, the emission lines observed have been in the visual part of the electromagnetic spectrum. This limits the number of usable lines, and introduces large systematic uncertainties in the measured ^4He abundances due to degenerate physical parameters in modeling the HII regions (particularly in electron density and temperature). Recent studies (Izotov et al. 2014) have proposed using the He I λ10830 infrared emission line to further reduce error. He I λ10830 has a strong electron density dependence that is expected to help minimize the impact of degenerate model parameters.

Aver et al. (2015) incorporate newly available observations of He I λ10830 into previous analysis. Using the HeBCD sample (a sample of low-metallicity blue compact dwarf galaxies collected to study helium abundances) of Izotov et al. (2014), they consider only observations for which all relevant visible He emission lines are seen. They ultimately use 15 objects with usefully clear He I λ10830 emission. The inclusion of the He I λ10830 line reduces the data set size for this analysis, but constrains the otherwise degenerate parameters so much better, that the smaller sample is acceptable. They find that the abundance errors on the model parameters are reduced by around 80%. When this data is extrapolated to determine a primordial abundance, they obtain a value[5] determined to 1.6%: $Y_p = 0.2449 \pm 0.0040$.

6. LITHIUM-7 CREATION AND ABUNDANCE

6.1. *Mechanisms*

Of the four reference primordial abundances in BBN modeling, the ^7Li abundance is the only one where the predicted values do not match up with observational data. This is often referred to as the "Lithium Problem," and is further addressed in sec.6.3. There are two primary BBN formation

[5] This is the $^4He/H$ value used by PRIMAT for comparison purposes.

mechanisms for ^7Li, both of which are dependent on the creation of ^7Be nuclei.

$$^3He + ^4He \rightarrow ^7Be + \gamma$$

While it is crucial in the production of primordial Lithium, ^7Be is not useful as a benchmark for testing BBN models. Like tritium, it is a radioactive isotope with a half-life much shorter than the age of the Universe, at about 53 days (Ohtsuki et al. 2004).

From here, ^7Li is created through the collision of a ^7Be with a neutron, or through electron-capture decay.

$$n + ^7Be \rightarrow ^7Li + p$$

$$e^- + ^7Be \rightarrow ^7Li + \nu_e$$

Heavier elements than lithium are not created in BBN due to the "lithium bottleneck." Simply put, there is no reasonably common nuclear reaction between the constituent nuclei established thus far that can produce a stable 8 or 5-nucleon ion, which is necessary for the fusion of heavier elements. In stellar nucleosynthesis, this bottleneck is overcome by a triple-alpha process, in which three ^4He nuclei collide at the same time. This is only possible due to the very high density in a star's core, and would not have happened at a reasonable rate for significant formation of heavier elements during BBN.

6.2. *Observational Values*

In theory, finding an observational value for ^7Li is actually relatively easy compared to the other BBN indicators. An estimation can be made from the photospheres of relatively metal-poor, unevolved stars in the stellar halo. It is easy enough to measure the ^7Li abundance in the photosphere of a given star. Using spectroscopic data, the line strength (equivalent width) of known ^7Li absorption lines is measured, and compared to the line strength of known Hydrogen lines (usually the balmer series). Turing this measured abundance into an estimated primordial ^7Li abundance is potentially tricky. In stars with large convection zones, much of the observable ^7Li is pulled deeper into the star. When the temperature is hot enough, the ^7Li is very quickly burned.

$$p + ^7Li \rightarrow 2^4He$$

Unevolved dwarf stars, by comparison, have very thin convective zones. So their photospheric ^7Li abundance is assumed to be about the same now as it was when they formed. This assumption is backed by the lithium plateau ("Spite plateau") in the observations of these Pop. II stars. Similarly to ^3He, it appears that, for a certain range of metallicities, the ^7Li abundance does not change as a function of metallicity. For some time, the value of the Spite Plateau was used as a bound.

Sbordone et al. (2010), however, presents observational evidence that for extremely metal poor stars ($[Fe/H] < -3$), there is no longer a plateau. Instead, they find a strong, positive, linear correlation between abundance and metallicity. Using the well-measured plateau value, and extrapolating back to very low metallicity based on the linear correlation, they estimate a primordial ^7Li abundance[6] of $10^{10}(^7Li/H)_P = 1.58 \pm 0.31$.

It is important to note that while this estimate is sound based on the data observed, there is not yet a physical explanation for the breakdown of the Spite Plateau (Sbordone et al. 2010). What is the ^7Li depletion mechanism at the time Pop. III stars that stopped as stars of metallicity $[Fe/H] > -2.8$ began to form? The breakdown of the plateau at lower metallicities is truly confounding.

6.3. *The Lithium Problem*

If the mysterious depletion mechanism creating the Spite plateau breakdown wasn't strange enough, it is also important to note that the current observationally obtained value for primordial ^7Li abundance is entirely too low, compared to model values. PRIMAT, for example, generally finds an estimate of $10^{10}(^7Li/H)_P = 5.623 \pm 0.247$ (Pitrou et al. 2018). A whopping 3.5 times greater than that observed in Sbordone et al. (2010). This is a huge difference, especially considering how well the other three indicators match up (see fig.1). There have been several proposed possible solutions to the lithium problem. These fall into three general categories: astrophysical, particle, and advanced solutions (Fields 2011).

6.3.1. *Astrophysical Solutions*

[6] This is the $^7Li/H$ value used by PRIMAT for comparison purposes.

It is possible the lithium problem is caused by an error in the measured primordial abundance of ^7Li. These solutions posit that the model values are sound, and that there is no error in ΛCDM or our understanding of particle physics. It is possible that there may be systemic errors in how the stellar ^7Li abundances of the Pop. II halo stars are measured. For starters, it is possible the base assumption that the current abundance is comparable to the plateau abundance is flawed. Beyond this, the abundance values are for the total lithium content over all ionization states, but the lithium in the stars is mostly singly-ionized. Additionally, the measurements include only one accessible ^7Li line (at 670.8 nm). These issues require the introduction of a sizable ionization correction that is exponentially dependent on star temperature. As much as astronomers wish stars were truly perfect blackbodies, they are not, and determining stellar temperature is nontrivial. It is therefore reasonably possible that an error in the correction factor tis a contributor to the lithium problem (Fields 2011).

6.3.2. *Particle Physics Solutions*

The next possible solution is an error in our understanding of particle/nuclear physics processes. It is reasonably possible that some error may come in via experimentally obtained (and poorly constrained) values required for nuclear reaction rates. While these reactions may be well understood in familiar contexts (i.e. the Sun), the conditions present at BBN are strange enough that errors in experimental values like nuclear cross-sections may contribute more to the lithium problem than otherwise expected. This is true for both the weak interactions and the reactions that build up light nuclei (especially the mass-7 production of ^7Be). It is also possible that these reactions contain resonances that are either previously unseen or not well studied. Such resonances could impact reaction rates in a way that may change the expected amount of primordial ^7Li (Fields 2011).

6.3.3. *Advanced Solutions (Beyond the Standard Model)*

There have also been more radical proposed solutions to the lithium problem, looking instead at our baseline understanding of cosmology. This assumes that both our observed lithium abundances and understanding of nuclear physics are correct enough, but we're working in the wrong cosmology. The first problem with this is that for the most part, these theories are very well founded, and often

have extensive observational and experimental evidence. This is especially true for ΛCDM , which even uses the primordial abundance of ^4He as one of its observational pillars. That being said, there are three general proposed solutions in this realm. The first is that dark matter decay and supersymmetry are the cause of the lithium problem. If dark matter does, in fact, decay, it is possible that the energy and particles potentially released by dark matter decay accelerated the destruction of mass-7 nuclei, leading to a smaller primordial ^7Li abundance. The second proposes that perhaps there are errors in some cosmological constants (the fine structure constant is of particular interest). It is perhaps even possible that some cosmological "constants" are not actually constant in time at all. The third says that maybe there is a fundamental problem with our standard cosmology. Such theories, however, would have to work with strong, observationally-grounded evidence that, at the moment, best points toward ΛCDM cosmology (Fields 2011).

7. MODELLING BBN IN PRIMAT

The PRImordial MATter (PRIMAT) program is one of the more well-used for the purposes of modeling BBN. PRIMAT is an updated version of a previous BBN modeling code (EZ_BBN) that was written in Fortran77. The new code is nicely contained in a Mathematica notebook. It is relatively simple, and user-friendly. To date, the source paper for PRIMAT (Pitrou et al. 2018) has over 130 citations. To obtain a copy of PRIMAT, fill out the form at the bottom of the PRIMAT website[7].

7.1. *Overview*

PRIMAT works by tracking the creation of 59 different isotopes through three different temperature periods immediately following the Big Bang. In simplest terms, it does so by integrating the relevant systems of differential equations defined by cosmology and nuclear physics from the big bang to well beyond the end of nucleosynthesis. In doing so, it tracks ion abundances through three different temperature phases.

[7] www2.iap.fr/users/pitrou/primat.htm

The high temperature phase corresponds with times ranging from about 0-1 seconds. This represents the time before freeze-out, when weak interactions between protons and neutrons were dominant. Through this integration time, PRIMAT follows only the proton and neutron abundances.

The middle temperature phase corresponds with times around 1-100 seconds after the big bang. This corresponds to a time frame in which the dominant reactions are the ones described above. During this integration phase, PRIMAT tracks the abundances of nine significant nuclei: n, p, d, t, ^3He, ^4He, ^7Be, ^6Li, and ^7Li.

The low temperature phase integrates from times around 100-50,000 seconds (significantly after the end of BBN). For this time period, PRIMAT tracks the abundances of 56 different ions, including the nine above. It should be noted that the isotopes beyond the four reference nuclei are not stable, and will decay between the time of BBN and the present day (the lithium bottleneck, sec.6.1).

7.2. *Results*

The PRIMAT code comes with a series of notebooks to serve different purposes, and includes a number of example calculations. The primary code (PRIMAT-Main.nb) comes set up to run a model for SBBN. The primordial abundance results of a simple model run can be found in column 2 of tab.1. The code also comes with an optional Markov Chain Monte Carlo error analysis. The results quoted in (Pitrou et al. 2018) include this additional step. An MCMC run will yield greater precision and give the user a sense of the error in the estimates, but at the cost of runtime. For context, a single run is said to take about 1 minute, whereas an MCMC can take hours or days.

The Main notebook also outputs a number of useful plots for analysis. Most significantly, there are several plots for observing the production of the various isotopes over time. Fig.2 shows a set of example plots for a single run.

7.2.1. *Examples Using a Nonstandard Model*

As mentioned previously, SBBN has essentially no free parameters. The input values for cosmological constants are well constrained by the assumed cosmology and astronomical observation. PRIMAT, however, also makes it possible for the user to model BBN for nonstandard cases. Two

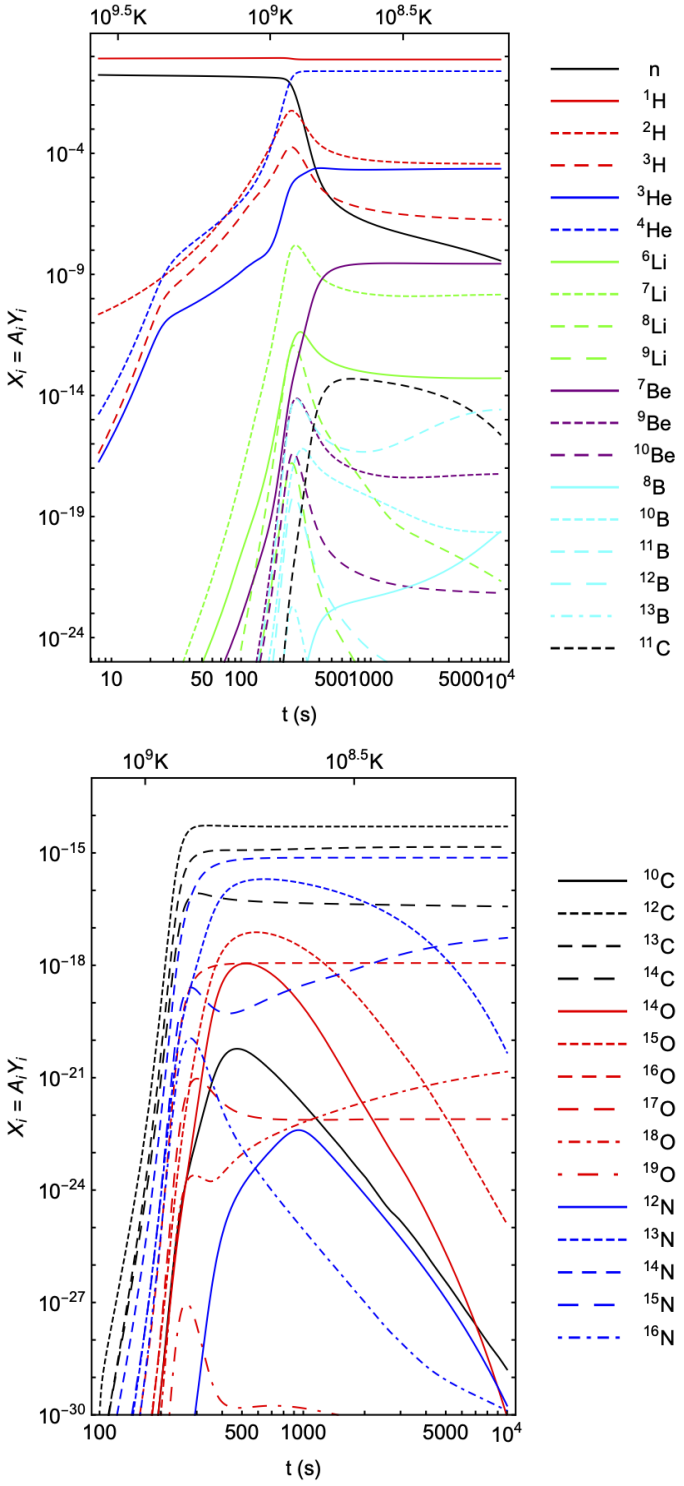

Figure 2. Relative mass abundances for a set of light (upper) and heavy (lower) isotopes over time.

Isotope	Primordial Mass Fraction	With MCMC (Pitrou et al. 2018)
n	7.174×10^{-11}	——
p	0.7527	——
d	3.670×10^{-5}	$(2.459 \pm 0.036) \times 10^{-5}$
^3He	2.329×10^{-5}	$(1.074 \pm 0.026) \times 10^{-5}$
^4He	0.2472	0.24709 ± 0.00017
^7Li	1.499×10^{-10}	$(5.623 \pm 0.247) \times 10^{-10}$

Table 1. The primordial abundance estimates for the relevant isotopes. The center column shows the values for a single PRIMAT run, while the right shows the results of a full MCMC run, reported in Pitrou et al. (2018)/

Isotope	Primordial Mass Fraction
n	2.087×10^{-10}
p	0.6944
d	6.129×10^{-5}
^3He	2.659×10^{-5}
^4He	0.3054
^7Li	2.890×10^{-10}

Table 2. The primordial abundance results for the nonstandard cosmology where $N_\nu = 9$.

example nonstandard cases are presented here. The first increases the number of neutrino flavors by a factor of three. The latter increases the baryon fraction Ω_b by an order of magnitude.

Tab.2 gives the modeled values of the primordial abundances when the number of neutrino generations N_ν is set to 9. Normally, based on the Standard Model of Particle Physics, this would be 3. There is a slight, but not insignificant difference in the values compared to the standard case.

Generally, it is easier to see the impacts of a nonstandard cosmology graphically. Fig.3 shows a small plot similar to those seen in fig.2. In this case, however, only the most relevant isotopes are graphed. For ease of comparison, this graph is shown alongside a similar graph of the standard case.

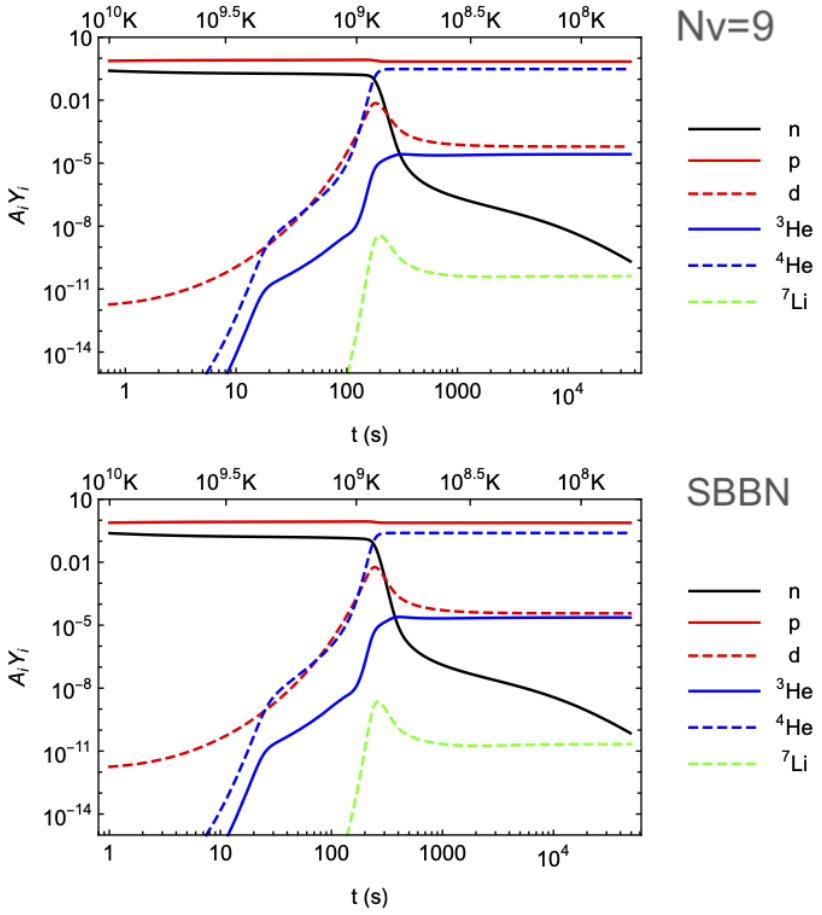

Figure 3. The results abundance graphs for the nonstandard cosmology where $N_\nu = 9$.

Comparing at the right sides of the graphs, it can be seen how the relative primordial abundances have shifted relative to each other in the $N_\nu = 9$ case.

An even clearer example of how a nonstandard cosmology changes primordial abundances can be seen when changing the baryon fraction, Ω_b. Ω_b is an observed value, and PRIMAT uses the results of Planck Collaboration et al. (2020), for their standard. Tab.3 and fig.4 show the results for a single model run wherein Ω_b is increased by a factor of 10 from the Planck Collaboration et al. (2020) model.

The clearest changes are in the neutron, deuterium, and ^7Li abundances, which drop off much more quickly in the high Ω_b case. That being said, there are also significant changes in the ^3He and ^4He abundances as well. These can be better seen graphically, comparing the plot of the high Ω_b case to the standard, as seen in fig.4

Isotope	Primordial Mass Fraction
n	1.499×10^{-17}
p	0.7326
d	1.048×10^{-8}
^3He	8.386×10^{-6}
^4He	0.2673
^7Li	3.667×10^{-16}

Table 3. The primordial abundance results for the nonstandard cosmology where Ω_b is an order of magnitude greater than the standard.

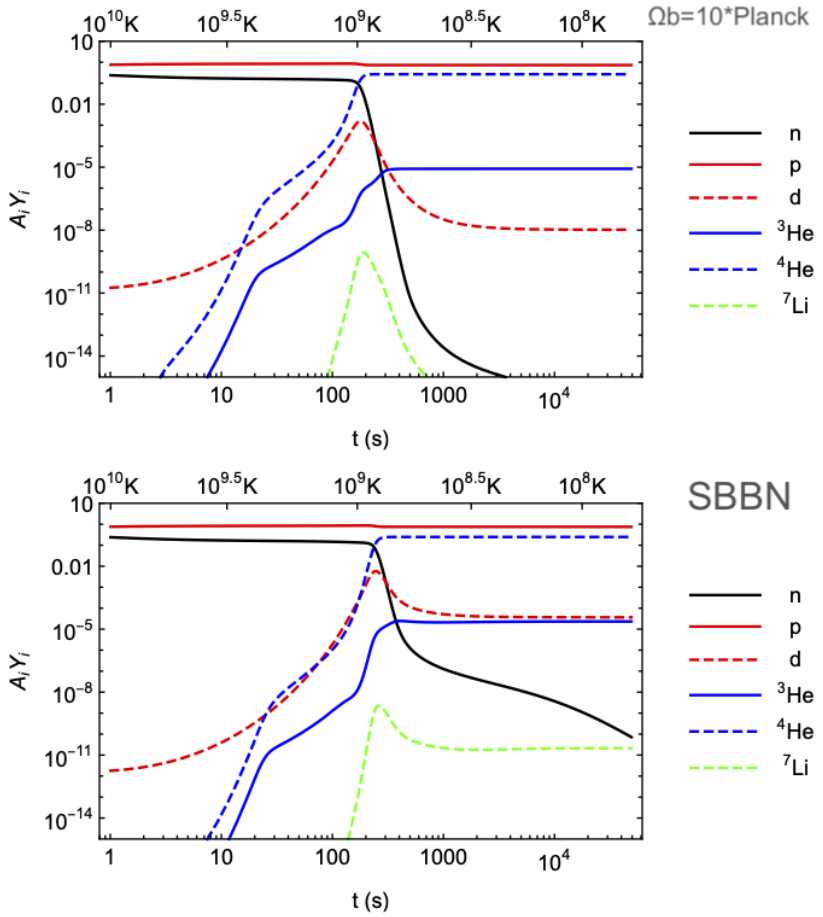

Figure 4. The abundance result graphs for the nonstandard cosmology where Ω_b is an order of magnitude greater than the standard.

REFERENCES

Pitrou, C., Coc, A., Uzan, J.-P., et al. 2018, PhR, 754, 1. doi:10.1016/j.physrep.2018.04.005

Cyburt, R. H., Fields, B. D., Olive, K. A., et al. 2016, Reviews of Modern Physics, 88, 015004. doi:10.1103/RevModPhys.88.015004

Davids, B. 2020, Mem. Soc. Astron. Italiana, 91, 20

Cooke, R. J., Pettini, M., & Steidel, C. C. 2018, ApJ, 855, 102. doi:10.3847/1538-4357/aaab53

Planck Collaboration, Aghanim, N., Akrami, Y., et al. 2020, A&A, 641, A6. doi:10.1051/0004-6361/201833910

Lucas, L. L., & Unterweger, M. P. 2000, Journal of research of the National Institute of Standards and Technology, 105, 4, doi:10.6028/jres.105.043

Bania, T., Rood, R. & Balser, D. 2002, Nature, 415 doi:10.1038/415054a

Rood R.T., Bania T.M., Balser D.S., Wilson T.L. 1998, Helium-3: Status and Prospects. In: Primordial Nuclei and Their Galactic Evolution. Space Sciences Series of ISSI, ed. Prantzos N., Tosi M., Von Steiger R., doi:10.1007/978-94-011-5116-0_19

Ohtsuki T., Yuki H., Muto M., Kasagi J. & Ohno K. 2004, Physical Review Letters, 93.

Aver, E., Olive, K. A., & Skillman, E. D. 2015, JCAP, 2015, 011. doi:10.1088/1475-7516/2015/07/011

Izotov, Y. I., Thuan, T. X., & Guseva, N. G. 2014, MNRAS, 445, 778. doi:10.1093/mnras/stu1771

Sbordone, L., Bonifacio, P., Caffau, E., et al. 2010, Chemical Abundances in the Universe: Connecting First Stars to Planets, 265, 75. doi:10.1017/S1743921310000244

Fields, B. D. 2011, Annual Review of Nuclear and Particle Science, 61, 47. doi:10.1146/annurev-nucl-102010-130445